Supporting Information

Accelerating ion/electron transport by engineering indium-based heterostructure toward large and reversible lithium storage

Experimental Section:

Materials

$In(OOCCH_3)_3 \cdot 2H_2O$ (AR) was purchased from Macklin Co., Ltd. Sublimed sulfur (AR) and thiourea (AR) were bought from Aladdin Co., Ltd. Polyethylene glycol-200 (PEG-200) was bought from Shanghai Yuanye Bio-Technology Co., Ltd. Anhydrous ethanol was produced by Tianjin Fuchen Chemical Reagent Co., Ltd. All of materials were used without further purification. Deionized water was produced using an ultrapure water dispenser (UPT-II-20T).

Material synthesis

Synthesis of ultrafine In_2O_3:S: 1 mmol $In(OOCCH_3)_2 \cdot 2H_2O$ and 1.5 mmol sublimed sulfur were suspended in 40 mL PEG-200 by stirring for 10 min and sonicating for 10 min. The suspension was stirred vigorously for 1 h at 180 °C and then cooled down naturally. The resultant precipitation was separated by centrifugation at 8,000 rpm, washed four times by deionized water and ethanol, and dried at 80 ^oC in vacuum oven.

Synthesis of heterostructured In_2O_3/In_2S_3: The prepared In_2O_3:S was annealed in Ar atmosphere at 600 ^oC for 2 h.

Synthesis of In_2O_3: The prepared In_2O_3/In_2S_3 was annealed in muffle furnace at 650 ^oC for 2 h.

Synthesis of In_2S_3: The prepared In_2O_3/In_2S_3 was heated at 600 ^oC for 2 hours under Ar atmosphere and reacted with the upstream H_2S gas produced by thiourea at 300 ^oC in a double-temperature-zone tube furnace.

Material characterizations

The phase structure of prepared samples was investigated by X-ray diffraction (XRD) using an ARL EQUINOX 3000 X-ray diffractometer (Thermo Fisher Scientific) with Cu Kα radiation (λ = 1.5418 Å) within the 2θ of 10–90°. The morphology of the In_2O_3/In_2S_3 heterostructure was observed using an ultra-high resolution scanning electron microscope (SEM, Verios 460 L, FEI) equipped with energy dispersive spectroscopy (EDX) at an accelerating voltage of 10 kV. Transmission electron microscopy image (TEM) and high-resolution transmission electron microscopy (HRTEM) with the ability to collect elemental information in high angle annular dark field-scanning transmission Electron microscopy (HAADF-STEM) mode were used to observe the morphology, composition and crystal phase (JEM-F200, JEOL). X-ray photoelectron spectroscopy (XPS) and valance-band XPS (VB-XPS) were conducted to element valance state in an Axis Ultra spectrometer (Kratos Analytical) using Al Kα radiation (hν = 1486.7 eV). The obtained binding energy was calibrated using the C 1*s* peak at 284.8 eV of adventitious carbon as the criterion. Raman spectroscopy (HORIBA JOBIN YVON S.A.S., France) was chosen to obtain the molecular structure and vibrational information of In_2O_3, In_2S_3 and In_2O_3/In_2S_3. Ultraviolet-visible (UV-Vis) absorption spectra were measured by a UV-Visible spectrometer (TU-1901, China) with a Φ 60 mm integration sphere. The test mode of UV-Vis curve is diffuse reflectance in this work, and the absorbance can be calculated by equation: A = 1 − R (%, reflectance). The electrical conductivity was measured on four-probe resistivity tester (ST2722-SZ, Suzhou Jingge Electronic Co., Ltd., China). 0.5 g powder was placed into Φ 12 mm sample groove of four-probe tester and a 20 MPa pressure was applied onto the powder sample. The resistivity of the sample under 20 MPa was recorded to calculate the electronic conductivity.

The valence band offsets (E_{VBO}) of In_2O_3/In_2S_3 heterostructure were determined from the energy separation between the core levels in the In_2O_3/In_2S_3 sample and the VBM to core level separation in pure In_2O_3 and In_2S_3.

$$E_{VBO} = E^{In_2O_3/In_2S_3}_{O1s} - E^{In_2O_3/In_2S_3}_{S2p_{3/2}} - \left(E^{In_2O_3}_{O1s} - E^{In_2O_3}_{VBM}\right) + \left(E^{In_2S_3}_{S2p_{3/2}} - E^{In_2S_3}_{VBM}\right)$$

$$E_{CBO} = E^{In_2O_3}_{g} - E^{In_2S_3}_{g} - E_{VBO}$$

Electrochemical Measurement

The slurry composed of active material, acetylene black and polyvinylidene fluoride (PVDF) with a weight ratio of 8:1:1 was coated onto Cu current collector by doctor blade and dried in a vacuum oven at 80 ^{o}C for 12 hours. The dried electrode was cut into Φ 12 mm discs for subsequent battery assembly. The CR2016 coin cells were assembled in a recirculating argon glovebox (H_2O: <0.01 ppm, O_2: <0.01 ppm). Lithium foil was used as the counter and reference electrode, and a glass fiber membrane (Whatman) was used as the separator, and the electrolyte (DoDo Chem Co., Ltd.) was 1 M $LiPF_6$ in ethyl carbonate (EC) and diethyl carbonate (DEC) (*w/w* = 50:50) with 10.0 % fluoroethylene carbonate (FEC) and 1.0 % vinylene carbonate (VC) as additives. The mass loading of the active materials was *ca.* 1–1.2 mg cm^{-2}. Galvanostatic charge/discharge performance and rate performance were performed by battery measurement system (LAND CT2001A, China) at a constant temperature of 25 ^{o}C within a potential window of 0.01–3.0 V (*vs.* Li/Li^{+}). The charge/discharge tests are conducted under constant current (cc) mode. Cyclic voltammetry (CV) tests were performed at scan rates from 0.2 mV s^{-1} to 5 mV s^{-1} within a potential window of 0.01–3.0 V (*vs.* Li/Li^{+}) used CHI760E (CH Instruments, China) electrochemical workstation. Electrochemical impedance spectra (EIS) were measured from 100 kHz to 0.01 Hz with an amplitude of 5 mV. The galvanostatic intermittent titration technique (GITT) was performed by pulse for 30 min at 0.05 A g^{-1} and relax for 60 min in the range of 0.01–3.0 V (*vs.* Li/Li^{+}).

The diffusion coefficient of Li^{+} can be estimated by the following formula.

$$D_{Li^+} = \left(\frac{RT}{\sqrt{2}\sigma A c n^2 F^2}\right)^2 = \frac{R^2T^2}{2\sigma^2 A^2 c^2 n^4 F^4}$$

Where R, T, A, c, n and F are the gas constant, absolute temperature, area of electrode, volumetric concentration of Li^{+}, number of electron transfer and Faradic constant. The σ is the Warburg coefficient

The complete Randles-Sevcik equation:

$$i_p = 0.4463 nFAcD^{1/2} v^{1/2} \left(\frac{\alpha nF}{RT}\right)^{1/2}$$

Where i_p, n, A, F, D, c, v, R, T and α are the peak current, number of transferred

electrons, electrode area, Faraday constant, diffusion coefficient, volumetric concentration of Li^+, scan rate, gas constant, absolute temperature and transfer coefficient, respectively.

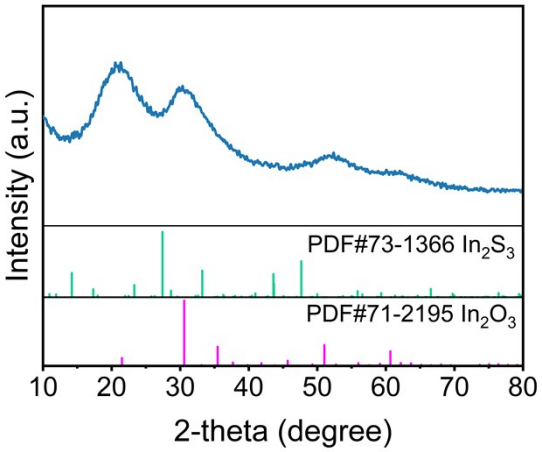

Fig. S1. The XRD pattern of In_2O_3:S.

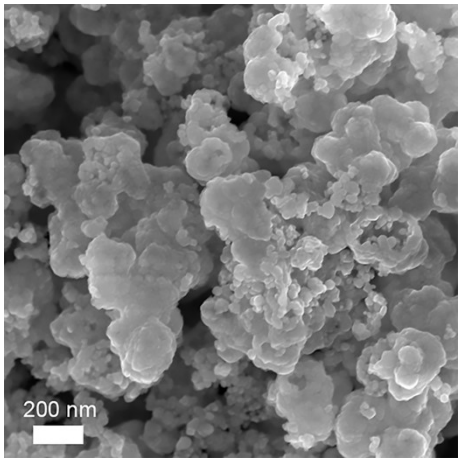

Fig. S2. The high-resolution SEM image of In_2O_3/In_2S_3.

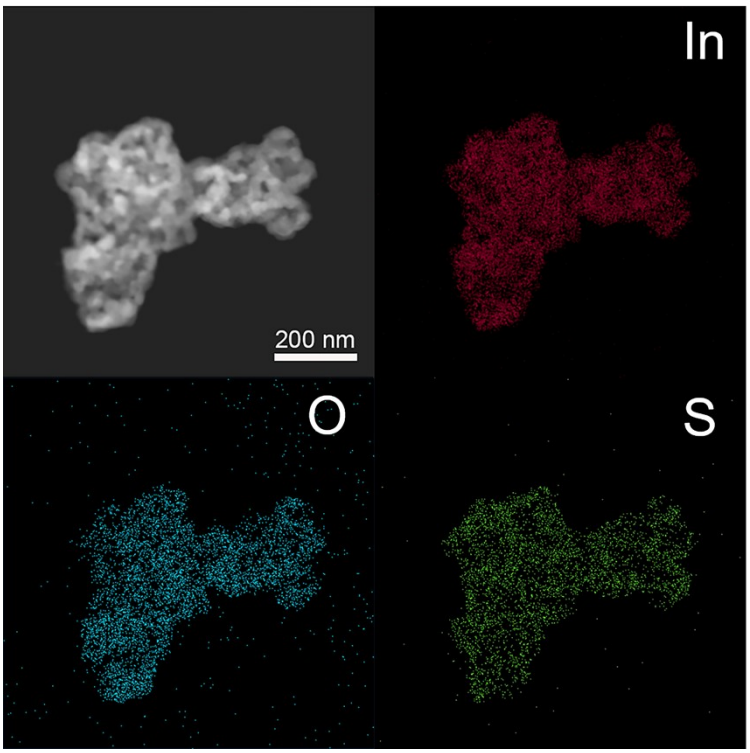

Fig. S3. The HAADF-STEM and EDX mapping images of In_2O_3/In_2S_3.

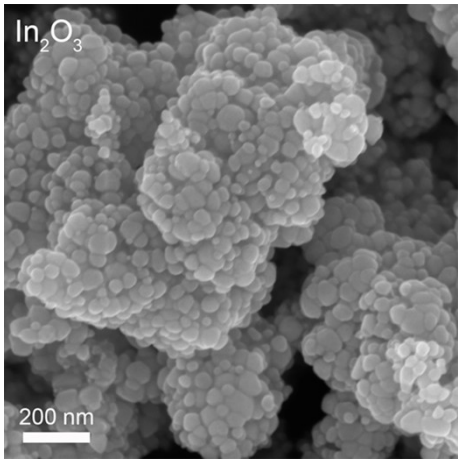

Fig. S4. The high-resolution SEM image of In_2O_3.

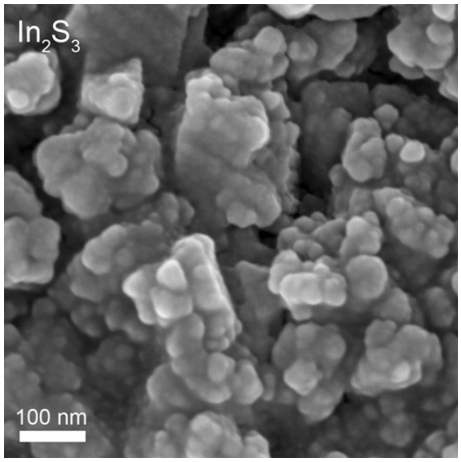

Fig. S5. The high-resolution SEM image of In_2S_3.

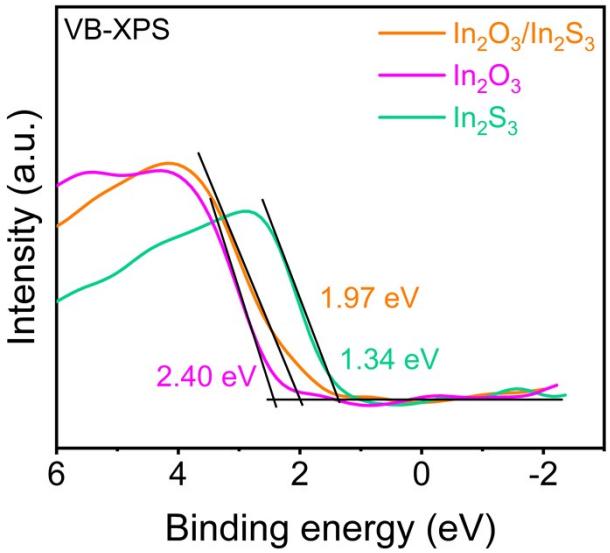

Fig. S6. The VB-XPS spectra of In_2O_3, In_2S_3 and In_2O_3/In_2S_3.

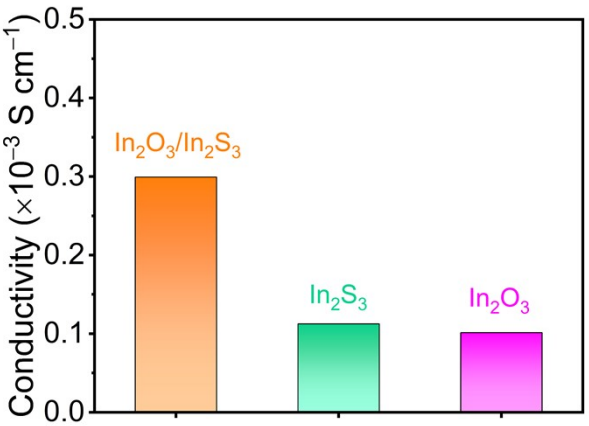

Fig. S7. The four-probe conductivity measurement of In_2O_3, In_2S_3 and In_2O_3/In_2S_3 heterostructure.

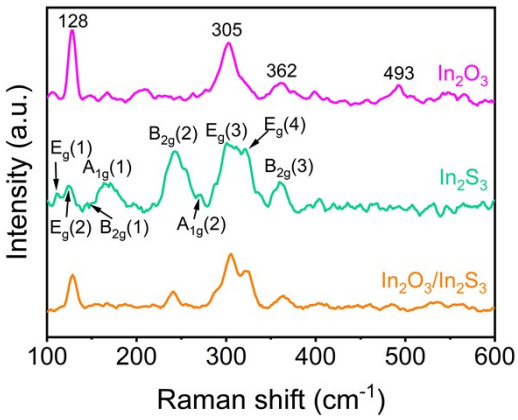

Fig. S8. The Raman spectra of In_2O_3, In_2S_3 and In_2O_3/In_2S_3 heterostructure.

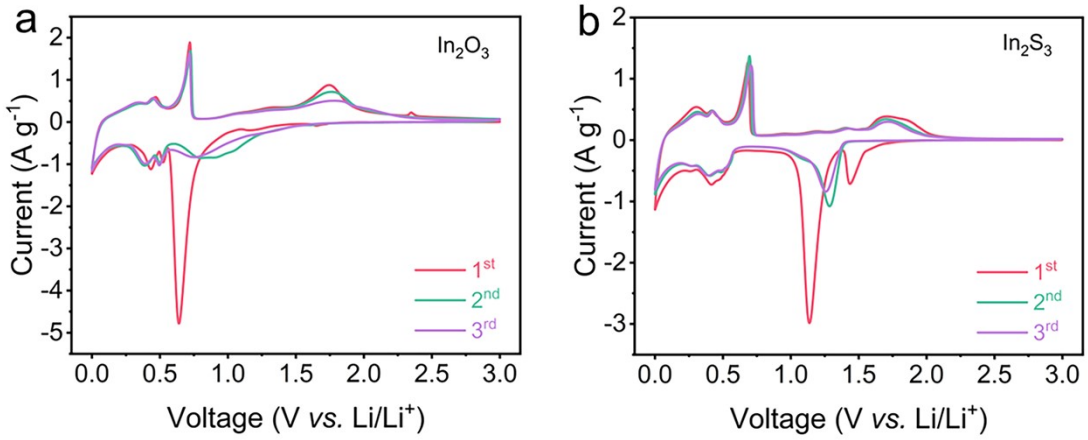

Fig. S9. The CV curves of **(a)** In_2O_3 and **(b)** In_2S_3 (scan rate: 0.3 mV s^{-1}).

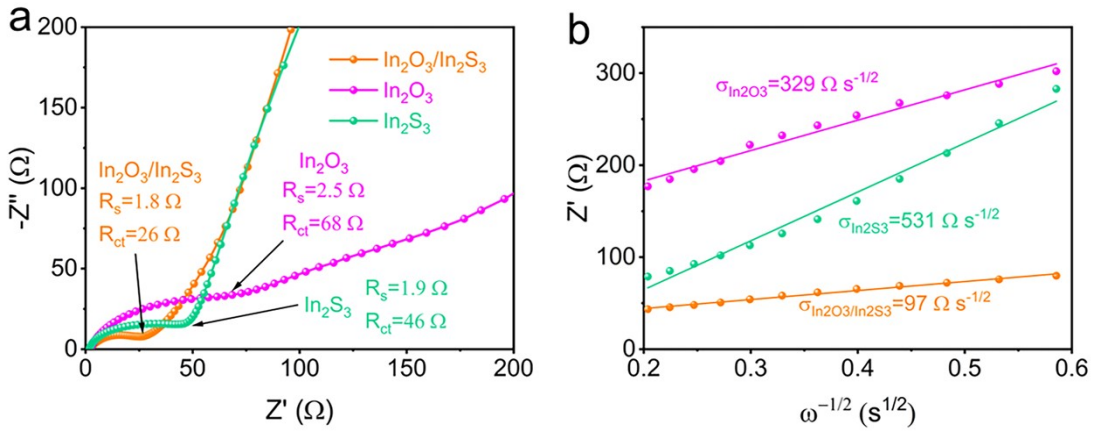

Fig. S10. (a) The EIS plots of the In_2O_3, In_2S_3 and In_2O_3/In_2S_3 electrode and corresponding fitting curves. **(b)** The linear fitting plots of Z' *vs.* $\omega^{-1/2}$.

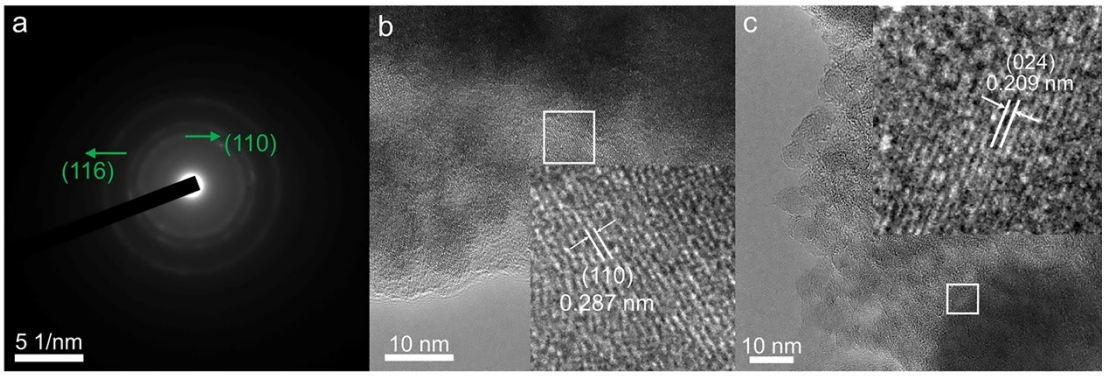

Fig. S11. (a) SAED and **(b-c)** high-resolution TEM image of In_2O_3/In_2S_3 electrode after the 1st charging into 3 V.

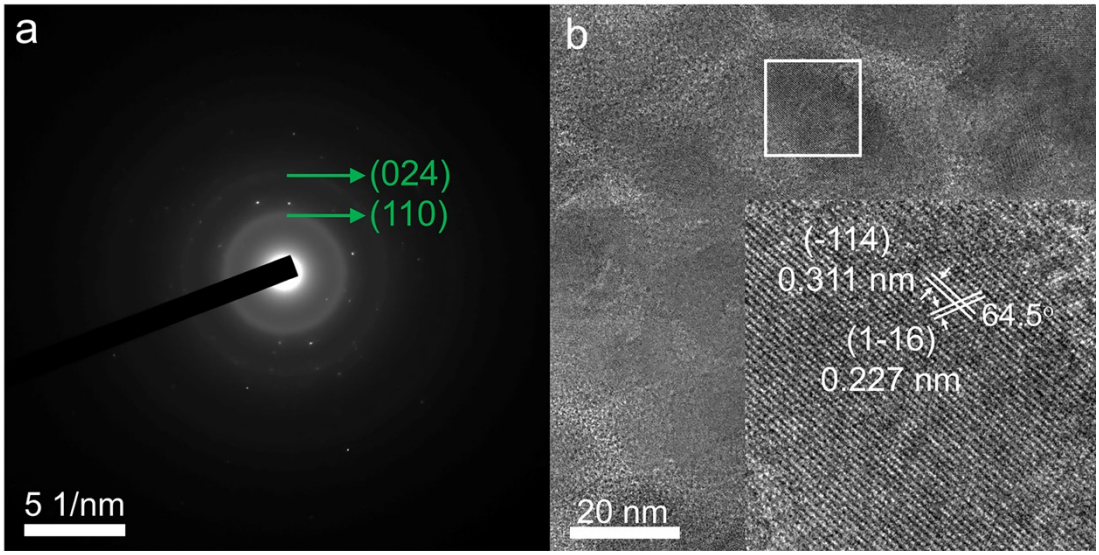

Fig. S12. (a) SAED and **(b)** high-resolution TEM image of In_2O_3/In_2S_3 electrode after the 5th charging into 3 V.

Table S1. EDX analysis of In_2O_3/In_2S_3 heterostructure.

Element	Line type	k factor	wt%	wt% Sigma	Atomic ratio
O	K	1.419	26.61	0.54	68.14
S	K	0.956	6.15	0.17	7.86
In	K	1.807	67.24	0.53	24.00
Total			100.00		100.00